Available online at www.sciencedirect.com

SCIENCE DIRECT®

Agricultural and Forest Meteorology 120 (2003) 69–82

AGRICULTURAL AND FOREST METEOROLOGY

www.elsevier.com/locate/agrformet

Estimated and measured DNA, plant-chromosphere and erythemal-weighted irradiances at Barrow and South Pole (1979–2000)

Susana Díaz[a,*], Don Nelson[b,1], Guillermo Deferrari[c,2], Carolina Camilión[d,3]

[a] CADIC/CONICET, Ushuaia, T. del Fuego, Argentina
[b] NOAA/CMDL, Boulder, CO, USA
[c] CADIC/NSF, Ushuaia, T. del Fuego, Argentina
[d] CADIC/IAI, Ushuaia, T. del Fuego, Argentina

Received 4 April 2002; received in revised form 17 April 2003; accepted 25 April 2003

Abstract

In the last two decades as a consequence of ozone depletion there has been an increasing interest in the study of biological effects of ultraviolet radiation (UV). Spectral instruments, which provide detailed information on UV environmental conditions, have been in use systematically only for little more than a decade. These time series are still relatively short and information on spectral historical irradiance levels is not available. Many efforts have been carried out in inferring this information from other available data sets. One of them has been the use of statistical models. Spectral irradiances are available at South Pole (90°00′S 0) and Barrow (71°18′N, 156°47′W) from the NSF UV Radiation Monitoring Program since 1991. In the present paper, daily-integrated biologically weighted irradiances for these sites are inferred back to 1979 using a multi-regressive model, obtaining time series that extend near the beginning of the Antarctic ozone depletion. These datasets are unique since the daily-integrated irradiances were calculated from irradiance measured hourly at the earth's surface. The biologically weighted irradiances are estimated from irradiance measured with broadband instruments, ozone, and solar zenith angles. From daily-integrated irradiance, monthly means were also calculated. The RMS errors between the estimated and measured daily-integrated irradiances range from 4.69 to 7.49% at South Pole and from 9.57 to 15.20% at Barrow, while the monthly mean errors vary from 2.07 to 3% and 2.95 to 3.91%, respectively. Completing the databases with spectral measurements, the resulting time series extend from 1979 to 2000. Analyzing monthly values an increase relative to 1979–1981 during all years is observed at South Pole. Largest increases are observed for DNA and plant-chromosphere weighted irradiances during October. Although at a lower rate, an increase is also observed at Barrow during the spring. Maximum monthly increase at South Pole during October is near 1200% relative to 1979–1981, while the increase at Barrow is near one tenth of that percentage. Daily-integrated irradiance shows that a slight increase was present during the spring at South Pole for the period 1979–1981

---

* Corresponding author. Fax: +54-2901-430644.
E-mail addresses: subediaz@speedy.com.ar (S. Díaz), dnelson@cmdl.noaa.gov (D. Nelson), defe@infovia.com.ar (G. Deferrari), carolinacamilion@hotmail.com (C. Camilión).

[1] Fax: +1-303-497-5590.

[2] Fax: +54-2901-430644.

[3] Fax: +54-2901-430644.

doi:10.1016/j.agrformet.2003.08.017

reflecting the beginning of the ozone depletion. Historical maximums of daily-integrated DNA weighted irradiance at South Pole (90°00′S, 0°00′) are about as large as summer maximums at San Diego (32°45′N, 117°11′W).

Keywords: Climate impacts; O_3; UV; Solar radiation; Irradiance

1. Introduction

Ultraviolet radiation (UV) plays a key role in several biological functions, sometimes detrimental (e.g. DNA damage, immunosupression, cataracts) and others beneficial (e.g. assimilation of Vitamin D, diminishing of risk of some internal cancers). As a consequence of the ozone depletion, a considerable number of studies have been performed to investigate the effect of increasing UV radiation on ecosystems.

Many investigations have been carried out to study the effects of UV radiation on human health and, terrestrial and aquatic ecosystems. Table 1 summarizes only a few of the long list of papers in the literature.

As a consequence of the large differences in the magnitude of the irradiance with wavelength, usually broadband measurements do not provide enough information to determine a relation between the radiation level and the effects on biological systems, which are mostly wavelength dependent. Hence, spectral irradiances and irradiance weighted with the appropriate action spectrum are important for biological studies.

Systematic measurements of UV performed with spectral instruments began in the late 1980s, after the discovery of the ozone hole (for example, in 1988 the NSF UV Radiation Monitoring Program started operation). Much longer time series of erythemal-weighted and pyranometer irradiances are available.

Recently, a multi-regressive model, which allows estimation of spectral and biologically weighted irradiances from broadband measurements (e.g. pyranometer) has been developed (Díaz et al., 2003).

Table 1
A brief list of studies addressing detrimental and beneficial effects of UV radiation

Effect	Reference
Action spectrum of UV-induced DNA damage	Setlow (1974)
UV effect on eggs and larvae of anchovy	Hunter et al. (1979)
Determination of urocanic acid (UCA) as chomophore for UV-induced immunosuppression	DeFabo and Noonan (1983)
Studies on human outdoor exposure to UVR	Sliney et al. (1990)
Determination of DNA as chomophore for UV-induced immunosuppression	Kripke et al. (1992)
UV effect on phytoplankton primary production	Smith et al. (1992)
Review effects of UVR on terrestrial plants	Tevini (1993)
UV effect on primary production	Vincent and Roy (1993)
UV-B effects on soybean	Caldwell et al. (1994)
Review effects of UVR on terrestrial plants	Teramura and Sullivan (1994)
UV-B biological changes in Antarctic water	Cabrera and Pizarro (1994)
UV effect on phytoplankton photosynthesis	Helbling et al. (1994)
UV effect on pelagic ecosystems	Williamson (1995)
Cornea absorption of the UVR below 300 nm lens absorption of the UVR below 370 nm	Merriam (1996)
Photokeratitis in humans. Environmental exposure to UVR (UV-B + UV-A)	Mc Carty and Taylor (1996)
UV effect on nanoflagellates	Sommaruga et al. (1996)
UV effect on pelagic ecosystems	Vernet and Smith (1997)
Review of UV-B effects on heathland species	Bjorn et al. (1997)
Review effects UVR on terrestrial plants	Rozema et al. (1997)
UV Effect on phytoplankton photosynthesis	Cullen and Neale (1997)
UV Effect on phytoplankton photosynthesis	Neale et al. (1998)
Plants DNA damage. Action spectrum more weight UV-B wavelengths and little participation of UV-A	Rousseaux et al. (1999)
UV-B effect on sphagnum and carex fen ecosystems	Searles et al. (1999)
Diminishing of risk of several internal cancers by UV-B exposure	Grant (2002)

The methodology and accuracy of the model are discussed in detail in the above-mentioned paper. In the present paper, the model is applied to obtain three biologically weighted irradiances (DNA damage, erythemal and plant-chromophore) back to 1979 at South Pole (90°00′S, 0°00′) and Barrow, Alaska (71°18′N, 156°47′W), and the time series of the estimated irradiance, completed with spectral measurements are then analyzed. Satellite data has been used to reconstruct ground irradiance time series (Cebula et al., 1994; Eck et al., 1995; Cebula et al., 1996; Li et al., 2000) but, cloud and albedo are still problematic. Also, satellite measurements are performed only once a day, then daily values are inferred only from one measurement. Both ground-based irradiance measurements (spectral and broadband) used in this paper are performed once an hour, then the daily-integrated values used to solve the model are calculated from these hourly data, providing more detailed information. Some other empirical and statistical models, which use ground-based irradiance measurements, have been developed (Ito et al., 1994; Bodecker and McKenzie, 1996; Fioletov et al., 2000), but none include the methodology and sites that we are considering in the present paper. Also, the methodology proposed in the statistical model applied here is very simple, the regression coefficients are determined using co-exiting measurements of spectral and broadband irradiance, total column ozone and solar zenith angle (which is calculated with any of the available algorithms). No other auxiliary data is necessary (e.g. cloud cover, pressure, etc.).

2. Methodology and data

2.1. Methodology

Ground-level radiation is a function of several factors: sun-earth distance, atmospheric gases and aerosols, solar zenith angle, clouds, altitude and surface albedo. Solar zenith angle and the Earth-Sun distance (geometric factors) are very important in determining irradiances at the earth's surface (e.g. the irradiance variations with time of the day, latitude, and season are the result of a change in the solar zenith angle). Total column ozone is the most important atmospheric gas affecting ground-level UV irradiances and clouds may produce large changes in the irradiance at the earth's surface.

Assuming that the variation in spectral or biologically effective irradiances may be considered as the product of the variation associated with clouds and geometric factors, and an attenuation factor related to ozone changes, a multi-regressive model was developed to infer spectral or biologically effective irradiances from solar zenith angle, total column ozone, and a proxy for cloud cover (Díaz et al., 2003). In this paper, pyranometer data are selected as a proxy for cloud cover. The pyranometer data also include information on geometric factors, albedo, and aerosols to some extent.

Pyranometers are broadband instruments that measure with a flat filter (no weighting function) wavelengths from 285 to 2800 nm. As a consequence of the much smaller values of solar irradiances in the UV-B (280–320 nm) related to the other bands, these instruments are not able to provide information of the UV-B or the biologically effective irradiances that are considered in this paper, unless their data are combined with other datasets.

Taking into account that an exponential relationship is observed between biologically effective irradiance and broadband data, which is a consequence of the dependence of the first one on total column ozone, while the irradiances measured with a pyranometer can be considered independent of this parameter, then, the proposed multivariate equation is:

$$y = a_1 x_1 + a_2 x_2 + a_3 x_3 + b \qquad (1)$$

where $y = \ln E$ (E is the biologically weighted daily-integrated irradiance); $x_1 = \ln E_\mathrm{b}$ (E_b is the broadband daily-integrated irradiance); x_2 is the total column ozone (daily value); x_3 is the solar zenith angle averaged daily value from sunrise to sunset (solar zenith angle smaller or equal to 90°), a_1, a_2, a_3 and b are the regression coefficients, determined using the least squares approach.

It was observed that smaller errors between estimated and measured values are obtained, particularly in winter months, when the model is solved for each month of the year, calculating twelve sets of coefficients, instead of one set of coefficients for all months. Calculating only one coefficient set, winter months present larger errors since these months do not contribute significantly when included with other

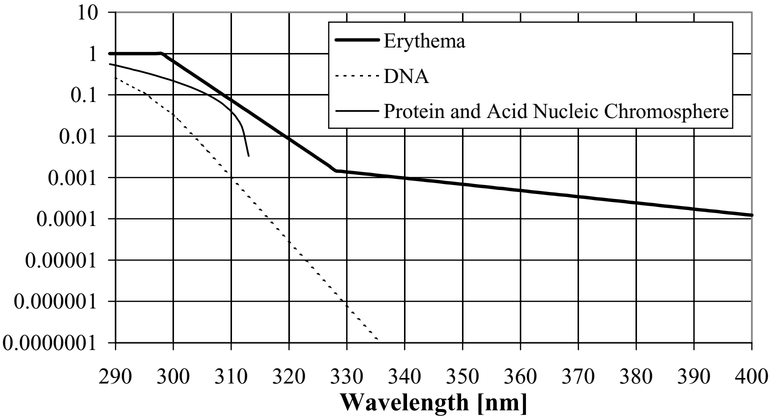

Fig. 1. Action spectrum for: DNA damage, plant-chromosphere and erythema (CIE). It can be observed that while for the first two action spectra the value falls strongly in the UV-B, the decrease for the erythema action spectrum in the UV-B is smaller, with an even smaller variation in the UV-A.

seasons at the moment of calculating the regression coefficients applying least squares.

In this paper, the multi-regressive equation is solved for three biologically weighted irradiances: (1) parameterization of DNA damage (Setlow, 1974), (2) plants related effects using a parameterization of Green et al. (1974) for biological response to UV-B when plant chromospheres are involved (Caldwell, 1971), and (3) erythemal (Mc Kinlay and Diffey, 1987). As it can be observed in Fig. 1, action spectra for DNA and plant-chromosphere show a more pronounced decrease with increasing wavelengths then, they are more affected by ozone changes. For the three action spectra, the model is solved for the period January 1993–December 1998 using Eq. (1), and then, the values are estimated back to 1979 by applying the regression coefficients determined for 1993–1998.

2.2. Data

Measurements of high spectral resolution irradiances are provided by SUV-100 spectroradiometers (Biospherical Instruments Inc., San Diego) of the NSF UV Radiation Monitoring Program (Booth, 1992–2000). These instruments are scanning, double-monochromator-based spectroradiometers with an irradiance collector that follows Lambert cosine law. They measure solar radiation at ground level, scanning across the ultraviolet and visible spectrum (280–605 nm) with a bandwidth of 1 nm. Data was collected hourly from the beginning of the Program until mid-1996 (or the beginning of 1997, depending on the site) and quarter-hourly since then to the present, in both cases between sunrise and sunset. The spectroradiometers have automatic response and wavelength calibrations performed once a day with internal Hg and Halogen–Tungsten lamps. External response calibrations are performed every 2 weeks with a 200-W external lamp. Periodically, usually once a year during site visits, external response and wavelength calibrations of all instruments in the network are performed with independent standard lamps, which are checked frequently by standard laboratories (Booth et al., 1998). The network is an effort of the Office of Polar Programs of NSF, which started operation in 1988. The stations are: South Pole, Mc Murdo and Palmer, in Antarctica; Ushuaia, Tierra del Fuego, Argentina; San Diego, California, USA; and Barrow, Alaska, USA (Booth et al., 1998).

Data is processed by Biospherical Instruments Inc., under contract of Raytheon Polar Services. Database 3 provides irradiances integrated at several bands and irradiances weighted by different action spectra, which are calculated as follows:

$$I = \sum_{\lambda_1}^{\lambda_2} (I_\lambda)(\lambda), \qquad W(\lambda) \tag{2}$$

where I is the biologically effective irradiance (μW/cm^2), $I_\lambda(\lambda)$ is the irradiance at wavelength λ (μW/cm^2/nm), and $W(\lambda)$ is the weighting function (action spectrum) (dimensionless), and λ_1 and λ_2 are the limit wavelengths. The summing is performed between 280 and 400 nm in 1 nm steps (Booth et al., 1998).

South Pole and Barrow were selected for the estimation of historical irradiances since they are the only two sites of the NSF UV Radiation Monitoring Program where well-calibrated pyranometer data, prior to the installation of the NSF network, are available.

Spectral measurements are performed for South Pole (90°S, 0) only from October to March and for Barrow (71°18′N, 156°47′W) only from March to September, due to polar night. Data collected under all weather conditions is used; thus the data include different cloud covers, solar zenith angles and albedo. Databases of spectral time series for both sites are available since 1991 to present with minor gaps. Uncertainty is wavelength dependent, but for the irradiances used in this paper it is estimated to be near ±6%.

Total column ozone is provided by NASA Goddard Space Flight Center (Mc Peters and Beach, 1996, 2001; Herman, 1998). Data are available from TOMS instruments (Total Ozone Mapping Spectrometers) on three different satellites back to 1979 (Nimbus-7, Meteor 3 and Earth Probe), with a gap between January 1995 and September 1996, winter gaps at South Pole and some minor gaps. TOMS instruments on satellites Nimbus-7 and Meteor 3 show a drift of 0.5% per decade, relative to ground-based Dobson measurements, while for Earth Probe the drift for July 1996 to April 2000 is 1.5%.

Pyranometer data collected by NOAA/CMDL at South Pole and Barrow are used for broadband irradiance. These pyranometers are of the double dome type, with a single black detector; and each pyranometer was characterized for angular and temperature response. The CMDL sensors were selected for optimal operation at high latitudes (Nelson, 2000). Data is available from January 1976 to December 1998 (with gaps in 1984 at Barrow and a few minor gaps). Pyranometers deployed by the NOAA/CMDL at these stations were characterized and calibrated at the NOAA/CMDL Solar Radiation Facility in Boulder Colorado. All calibrations are traceable to absolute cavity radiometers, which are in turn traceable to the World Radiometric Reference (WRR) in Davos, Switzerland (Nelson, 2000).

After estimated biologically weighted irradiances were calculated from 1979 to 1998, the gap produced by the lack of ozone satellite measurements from December 1994 to June 1996, the period 1998–2000, and March 1994 at Barrow, are completed with biologically weighted irradiance obtained from spectral measurements (NSF UV Radiation Monitoring Program, SUV-100). Then, a complete time series from 1979 to 2000 is reconstructed for analysis.

3. Results and discussion

As pointed out in a previous section, simultaneous data of biologically weighted and broadband irradiances are necessary to obtain the regression coefficients of Eq. (1). The model is solved for the period 1993–1998 and the RMS error for daily-integrated irradiance is shown in Table 2. The error remains at acceptable levels for the purposes of this paper and shows larger values at Barrow as a consequence of cloudier skies. Then, monthly means are calculated from the measured and estimated daily-integrated values, and the error is determined (Table 3). The equation of the regression lines relating measured and estimated values exhibit negligible effects of systematic over or under estimation of the model (b near zero and slope near 1). Fig. 2a and b show the scatter plots for measured and estimated daily-integrated and monthly mean values for erythemally weighted irradiance at Barrow. As a reference, it may be mentioned that for well-characterized spectroradiometers, measured

Table 2
RMS error biologically weighted daily-integrated irradiance (1993–1998)

	DNA (%)	Plants (%)	Erythema (%)
South Pole	7.49	7.45	4.69
Barrow	15.20	14.13	9.57

Table 3
RMS error biologically weighted monthly mean daily-integrated irradiance (1993–1998)

	DNA (%)	Plants (%)	Erythema (%)
South Pole	3.00	2.86	2.07
Barrow	3.91	3.75	2.95

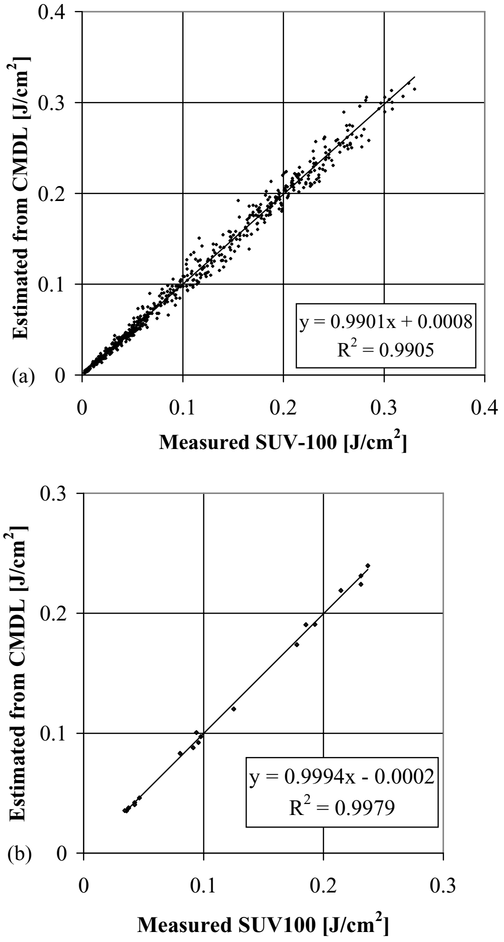

Fig. 2. Scatter plot of estimated and measured erythemal weighted irradiance for Barrow, for the period 1993–1998 (a) Daily-integrated irradiance, (b) monthly mean of daily-integrated irradiance.

erythemal irradiance may show an uncertainty of ±6% (Bernhard and Seckmeyer, 1999), and for biometers the uncertainty can be much larger (Bais et al., 2001).

Irradiance in the band 337.5–342.5 nm can be used as a proxy for clouds (Díaz et al., 2000), since this band is not affected by changes in the ozone column. Therefore, irradiances for this band are also estimated following the described procedure, and are included in the analysis to evaluate cloud effects. The resulting RMS errors for this analysis are shown in Table 4, and they are smaller than the errors computed for the biologically weighted irradiances. This is in good agreement with previous results (Díaz et al., 2003), which show a decrease in the error when inferring longer wavelength irradiance from pyranometer measurements.

Table 4
RMS error 337.5–342.5 nm monthly mean and daily-integrated irradiance (1993–1998)

	Daily-integrated (%)	Monthly mean (%)
South Pole	3.31	1.40
Barrow	8.40	2.59

Monthly mean daily-integrated DNA, plant-chromosphere and erythemally weighted irradiance estimated from pyranometer and obtained from spectral measurements SUV-100 are shown in Fig. 3. Both datasets exhibit very good agreement at the period where they overlap. While an increase is clearly observed since 1987 at South Pole, especially for DNA and plant-chromosphere, no significant increase is evident in these graphs at Barrow.

The monthly variation relative to the corresponding monthly average for years 1979–1981 is computed for the three biologically weighted irradiances at both sites, and the results are shown in Fig. 4. A gradual increase is observed at South Pole, with a larger value for DNA and plant-chromosphere weighted irradiances. This should be expected as a consequence of the larger weighting factors of these action spectra at wavelengths more sensitive to ozone variations. The main peaks are observed at 1987, 1993, and 1997 with values near 320, 650 and 1200%, in agreement with low monthly-mean ozone values. Most months show a considerable positive variation and only a few small negative values are observed. At Barrow, smaller negative and larger positive values are observed after 1985, with the highest increases after 1990, although with values much lower than those at South Pole (near 110% versus 1200%). The most affected months are October and November at South Pole and March and April at Barrow, as could be expected in accordance to ozone depletion. Fig. 5 shows the variation for the above-mentioned months. October shows an increase similar to that observed for the complete time series (Fig. 4a), while in November an increase is observed from 1979 to 1987 and then increases remain about one third to one-fourth of those for October. At Barrow, during March, a considerable increment relative to 1979–1981 is evident since 1987, with an

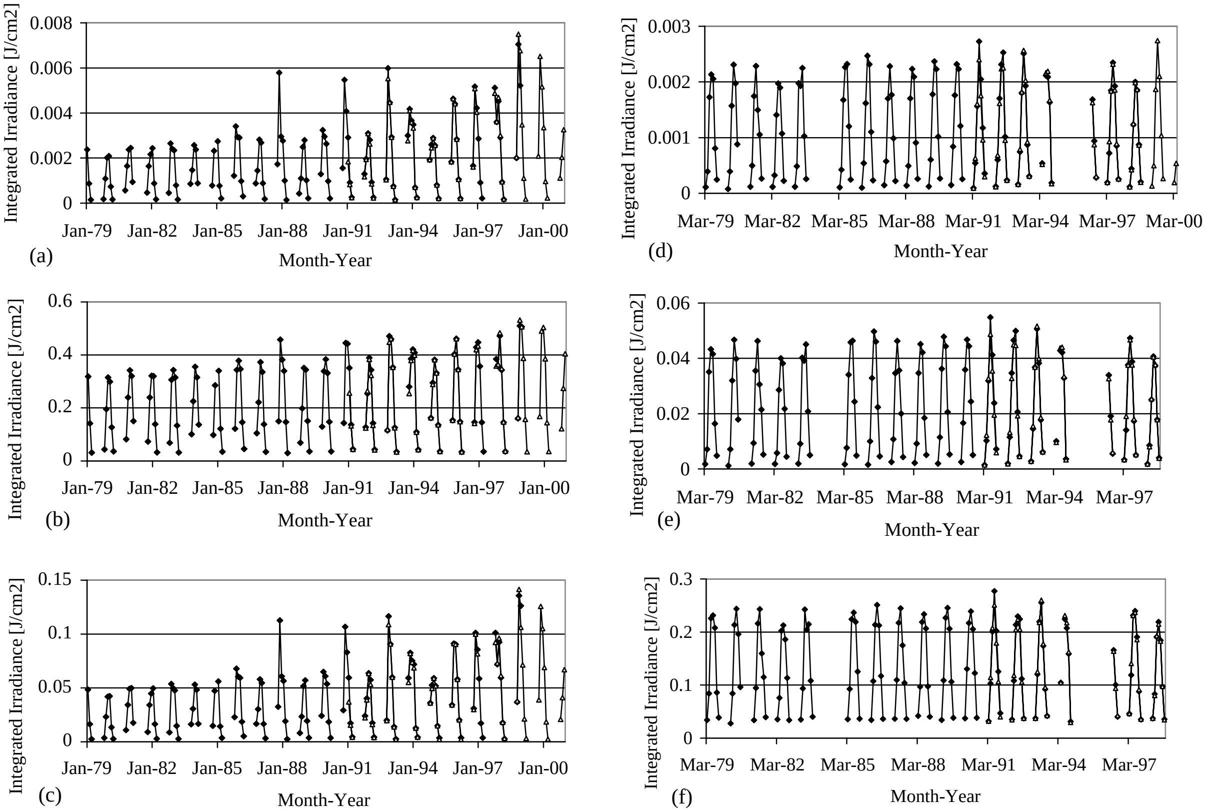

Fig. 3. Monthly mean daily-integrated irradiances, 1979–2000. For South Pole: (a) DNA, (b) protein and nucleic acid chromospheres, (c) erythemal. For Barrow: (d) DNA, (e) protein and nucleic acid chromospheres, (f) erythemal. Irradiances estimated from pyranometer (diamonds) and obtained from SUV-100 measurements (triangles) show very good agreement, as may be observed in the periods that overlap. Data for South Pole are available each year from October to March and in Barrow from March to September.

increasing trend, while for April, increases in both the higher and the lower values occur between 1990 and 1996. This more erratic variation at Barrow is in accordance with ozone depletion in the Arctic, which has not been present systematically each year (WMO, 1999). Also, analyzing monthly-mean total column ozone and 337.5–342.5 nm irradiance, there is good agreement between years when total column ozone is low and biologically weighted irradiance are high, while the 337.5–342.5 nm band for those years does not show significant changes relative to other years.

Mean and standard deviation of daily-integrated, DNA-weighted irradiance and 337.5–342.5 nm for 1979–2000 are shown for each Julian Day in Fig. 6. The mean daily-integrated irradiance for 1979–1981 is also included for reference. There are several features to discuss in these graphs.

(a) $\mathrm{Mean}_{79\text{–}81}$ DNA weighted irradiance at South Pole shows values near ($\mathrm{Mean}_{79\text{–}2000} - \sigma$), where σ is the standard deviation, for all Julian days. At Barrow it shows more erratic values, except for the spring where it is most of the time near the ($\mathrm{Mean}_{79\text{–}2000} - \sigma$). This more erratic behavior is, in general, a consequence of cloudier skies.
(b) At the end of November and beginning of December ($\mathrm{Mean}_{79\text{–}2000} + \sigma$) DNA weighted irradiance at South Pole shows values around 50% larger than ($\mathrm{Mean}_{79\text{–}2000} + \sigma$) at the summer solstice, as a consequence of low ozone values produced by the “ozone hole”.
(c) $\mathrm{Mean}_{79\text{–}81}$ DNA weighted irradiance at South Pole shows slight increases in the irradiances during the spring. This is consistent with a small

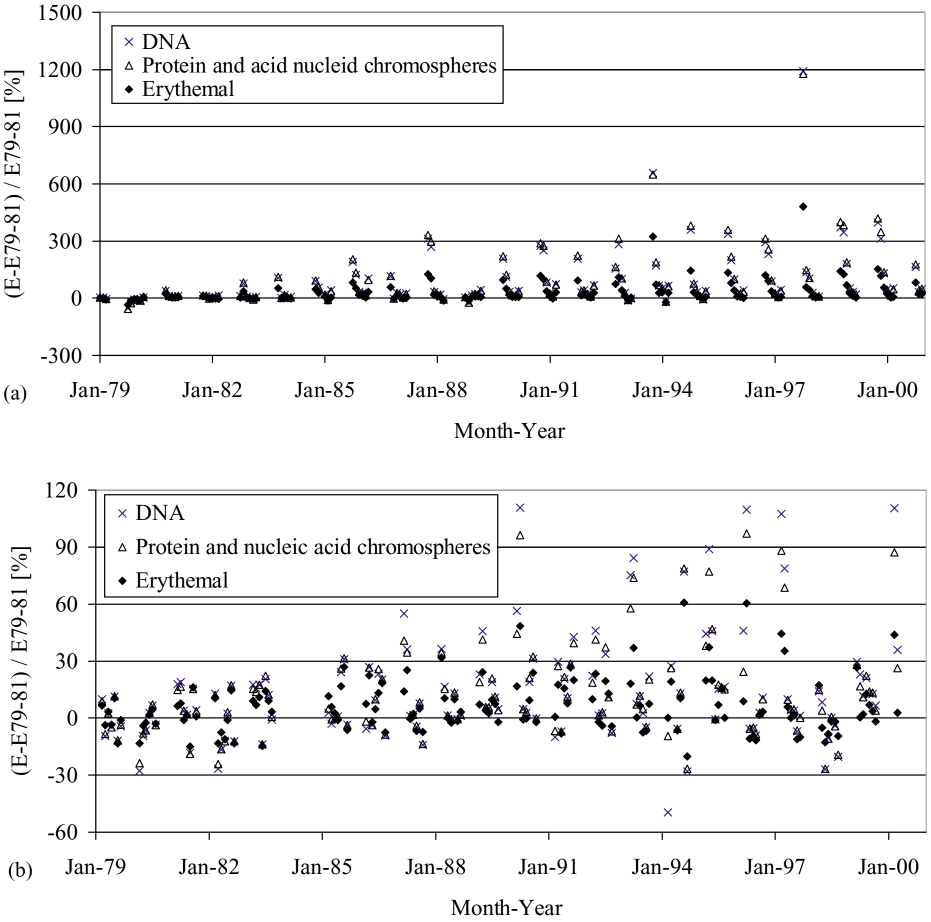

Fig. 4. Variation in monthly mean daily-integrated irradiances relative to mean 1979–1981 for (a) South Pole, (b) Barrow.

depletion of the total column ozone, which began to be present at that time (mainly in 1980 and 1981). Larger irradiance values persisting until later in spring (even early December) are observed for the values of $\text{Mean}_{79\text{–}2000}$, which reflect low total column ozone values and which is consistent with a later break up of the vortex.

(d) Fig. 7 shows modeled clear sky daily-integrated irradiance at South Pole for the 337.5–342.5 nm band as a function of Julian Day. The values are calculated using a disort model with albedo 0.9. The mean value for 1979–1981 is included in the same figure for reference. Comparing Fig. 6b with Fig. 7 it may be concluded that there is a predominance of clear skies at South Pole. Also, Fig. 6b shows almost no inter-annual variation for this parameter. This observation is in agreement with the results obtained in the analysis of the SUV-100 measured irradiance during the period 1991–1997 (Díaz et al., 2003). It can be concluded that all the inter-annual variation in Fig. 6a can be attributed to ozone variation. The previous result also suggests that the drift between the instrument calibrations and the model is negligible when using the regression coefficients developed for 1993–1998 to infer values for the period 1979–2000.

(e) The daily-integrated irradiance 337.5–342.5 nm band at Barrow (Fig. 6d) shows more variability, in accordance with cloudier skies, and values are similar to, or lower than values at South Pole,

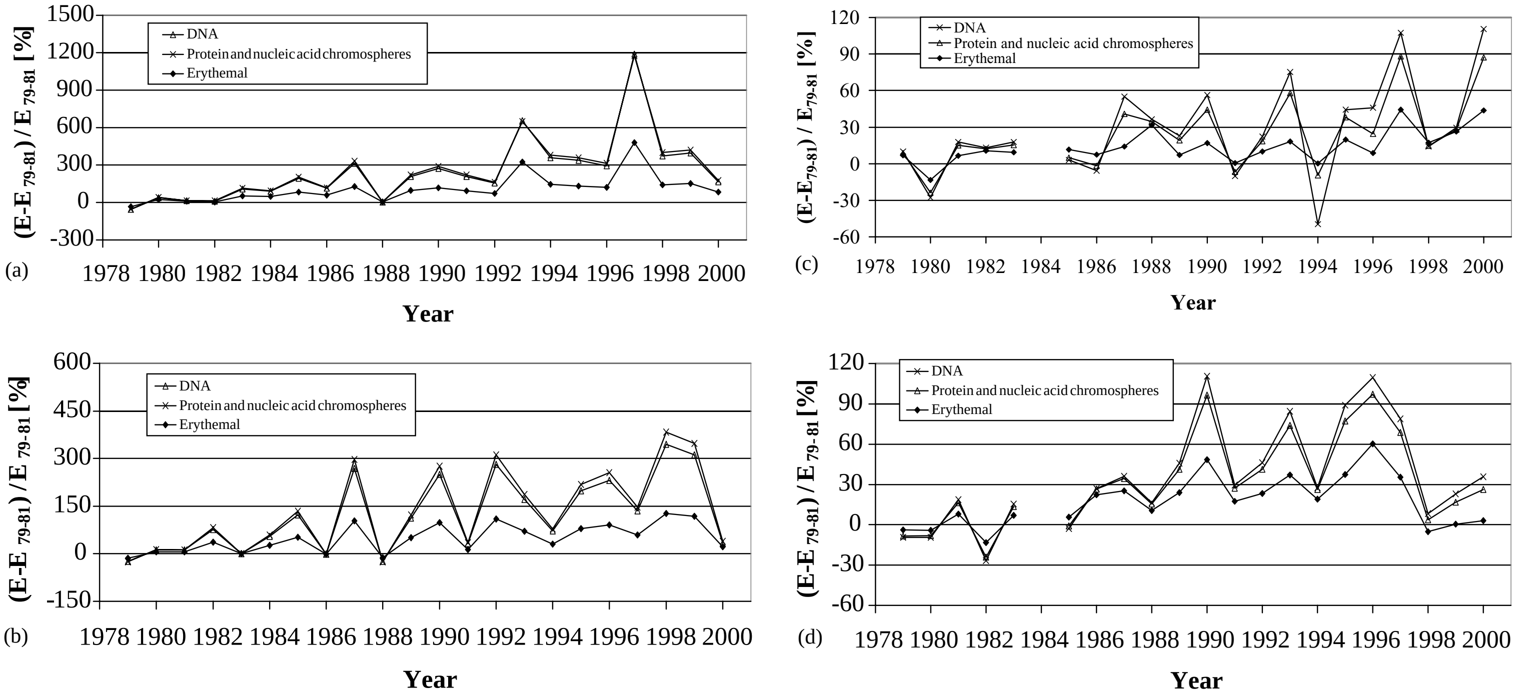

Fig. 5. Variation in monthly mean daily-integrated irradiance relative to mean 1979–1981 for (a) South Pole, October; (b) South Pole, November; (c) Barrow, March; (d) Barrow, April.

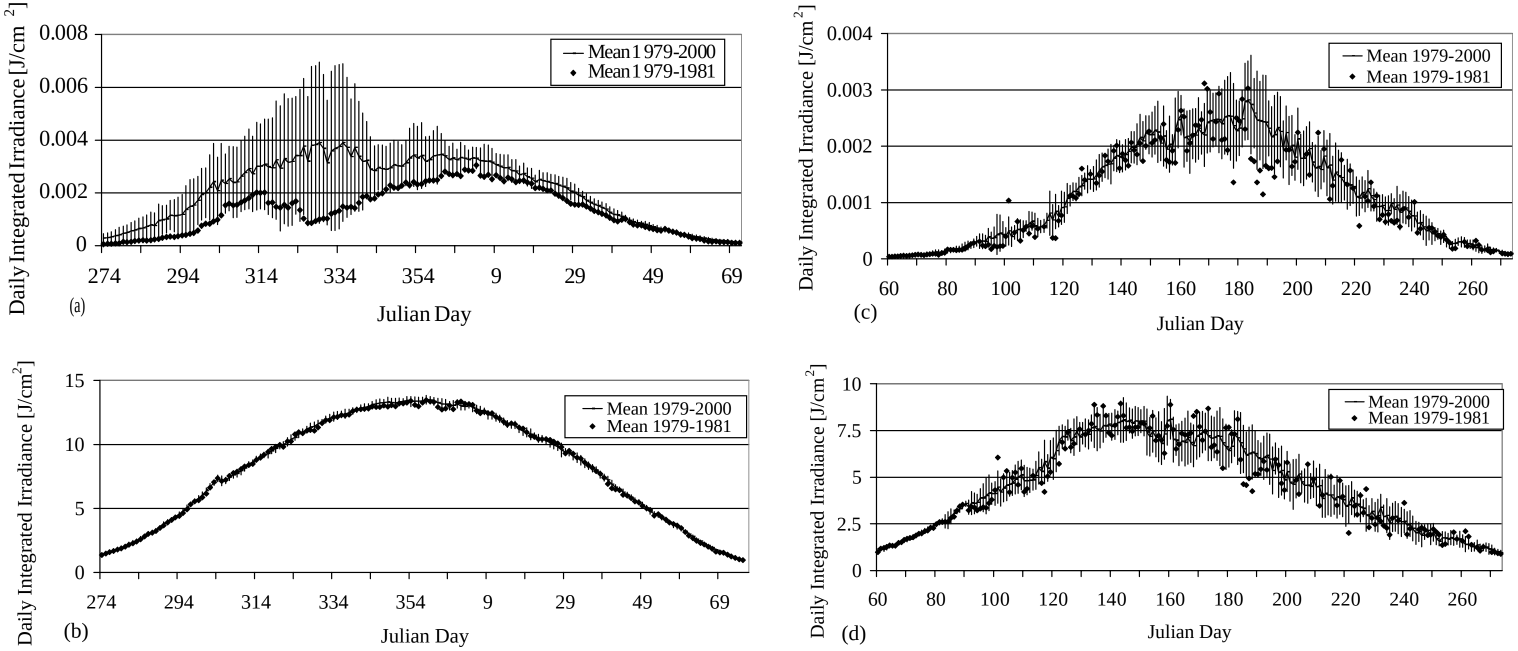

Fig. 6. Mean and standard deviation 1979–2000 and mean 1979–1981 of daily-integrated irradiance (a) South Pole DNA, (b) South Pole 337.5–342.5 nm, (c) Barrow DNA, (d) Barrow 337.5–342.5 nm.

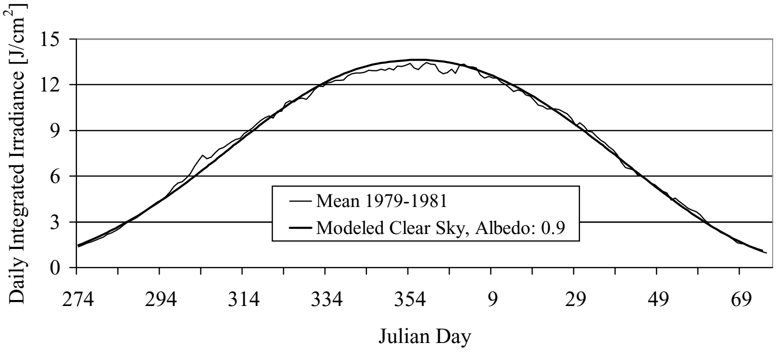

Fig. 7. Modeled clear sky irradiance 337.5–342.5 nm at South Pole and mean value 1979–1981 for the same band. A disort mode was used to calculate the clear sky values, with albedo 0.9.

mainly as a consequence of the smaller number of daylight hours, and somewhat because of cloud contributions.

(f) In spite of its latitude, DNA damaging irradiance $\text{Mean}_{79\text{–}2000}$ at South Pole during spring and summer is similar to, or exceeds, the corresponding values at Barrow, and ($\text{Mean}_{79\text{–}2000} + \sigma$) at South Pole are nearly twice the values at Barrow. Comparing $\text{Mean}_{79\text{–}81}$ at South Pole with $\text{Mean}_{79\text{–}2000}$ at Barrow, if may be inferred that the effect is mainly a result of the ozone depletion, with a smaller contribution of the number of daylight hours and cloud.

Historical maxima (1979–2000) of daily-integrated DNA weighted irradiance for Barrow and South Pole are shown in Fig. 8. Since these two sites are places with no great interest for the agriculture and forest community, we added historical maximum (1992–1997) for San Diego (32°45′N, 117°11′W), which were obtained from spectral measurements of the NSF network. Irradiance at San Diego serves

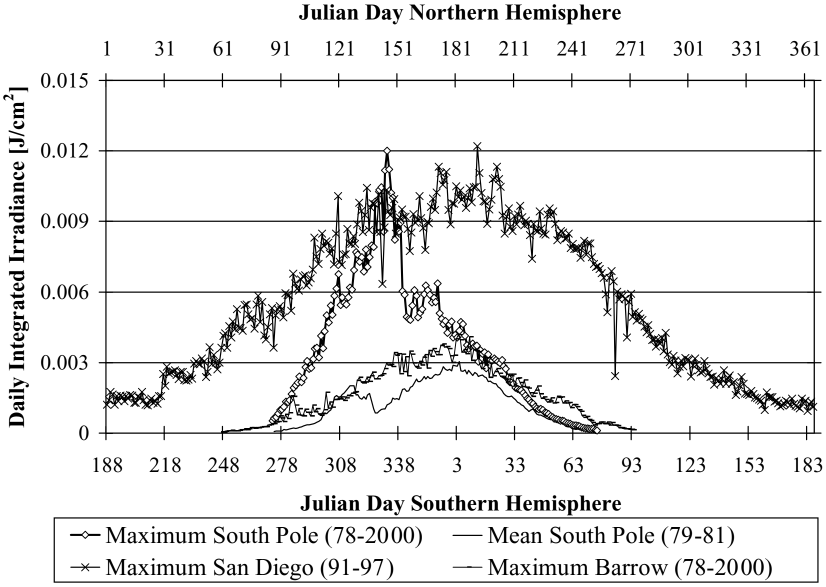

Fig. 8. Historical maximum of daily-integrated DNA weighted irradiance as a function of Julian Day at South Pole, San Diego, and Barrow compared to the mean for South Pole.

also as a reference level for a mid-latitude site where ozone depletion is mild compared to polar regions. $\mathrm{Mean}_{79\text{–}81}$ for South Pole is also included. In this figure, it is observed that:

(a) Maximum daily-integrated irradiance at the end of spring at South Pole exhibits values similar to those during the summer at San Diego. Since the number of daylight hours at South Pole is almost twice the number at San Diego in the summer, instantaneous values would show lower values at South Pole than at San Diego.

(b) Peak historical maximum irradiances at South Pole exceed by nearly 70% those obtained for $(\mathrm{Mean}_{79\text{–}2000} + \sigma)$, and are related to low ozone events (159 Dobson Units) during periods of small solar zenith angles (Julian day 333, 1998). (Total column ozone is measured in Dobson Unit (DU), one Dobson Unit is a height of one millimeter of pure gaseous ozone at 0 °C and 1013 hPa.)

(c) During spring and part of the summer, maximum values at South Pole exceed those at Barrow, as pointed out in the analysis of mean values, this effect is the result of ozone depletion.

4. Conclusions

A multi-regressive model was applied to infer daily-integrated biologically weighted irradiance from broadband instrument (pyranometer) measurements, total column ozone and solar zenith angles, at Barrow and South Pole. The model was solved for the period 1993–1998 for three different action spectra and a UV-A narrow band (used to analyze the effect of clouds), with very good agreement between estimated and measured values (RMS error below 15.20% for daily-integrated values and below 3.91% for monthly-mean of daily-integrated irradiances).

The biologically weighted irradiances were estimated from 1979 to 1998, the gap produced by the absence of satellite ozone data and the period 1998–2000 was completed with data obtained from the spectroradiometer SUV-100 (NSF UV Radiation Monitoring Program).

These reconstructed time series are unique, since daily-integrated values were obtained from hourly ground-based measurement of irradiance.

Analyzing daily-integrated values of the resulting time series an increase in the irradiance relative to the mean for the period 1979–1981, is observed. The most-affected months are October and November at South Pole and March and April at Barrow, consistent with ozone depletion. The increase is considerably larger at South Pole (maximum 1200%) than at Barrow (maximum 110%), as could be expected. In both cases the observed increase is much larger than the error of the model and measurements, which makes the results statistically significant. Peak values of daily-integrated DNA weighted irradiance at South Pole (90°00′S, 0°00′) during late spring are similar to summer values at San Diego (32°45′N, 117°11′W), as a consequence of ozone depletion and number of daylight hours.

At South Pole, mean DNA-weighted daily integrated irradiance for the period 1979–1981 shows values near $(\mathrm{Mean}_{79\text{–}2000} - \sigma)$, where σ is the standard deviation, for all Julian days. A small increase in the DNA irradiance, consistent with slight ozone depletion in 1980 and 1981, is observed during spring in the $\mathrm{Mean}_{79\text{–}81}$ at South Pole. Comparison of time series for 1979–1981 with 1979–2000 shows larger irradiances during the spring and that these are present at a later time in this season in the second time series, which reflects the increase of ozone depletion and later break up of the vortex.

Analysis of irradiance in the UV-A band (337.5–342.5 nm), used to analyze cloud effect, shows that the inter-annual variability in this parameter is negligible at South Pole. This analysis also shows that there is no significant drift between the instrument calibrations, nor drift in the irradiance values, as a consequence of the model calculations.

Acknowledgements

This publication was partially supported by the CRN-026 of the Inter-American Institute for Global Change. The authors want to thank Dr. P. Penhale and NSF Polar Programs, and CADIC/CONICET for their support to perform this study. They also want to thank Mr. C.R. Booth and the UV Group, Biospherical Instruments Inc (BSI), San Diego for providing the irradiance databases and Drs. R. Mc Peters and J. Herman, NASA GSFC for providing total column ozone. In addition, the authors are grateful to

NOAA/CMDL for providing the broadband irradiance data.

References

Bais, A., Topaloglou, C., Kazadzis, S., Blumthaler, M., Schreder, J., Schmalweiser, A., Henriques, D., Janouch, M., 2001. Report of the LAP/COST/WMO intercomparison of erythemal radiometers (Thessaloniki, Greece, 13–23 September 1999), World Meteorological Organization, Global Atmosphere Watch, Report No. 141.

Bernhard, G., Seckmeyer, G., 1999. Uncertainty of measurements of spectral solar UV irradiance. J. Geophys. Res. 104, 14321–14345.

Bjorn, L.O., Callaghan, T.V., Johnson, I., Lee, J.A., Manetas, Y., Paul, N.D., Sonesson, M., Wellburn, A.R., Coop, D., Heide-Jorgensen, H.S., Gehrke, C., Gwynn-Jones, D., Johanson, U., Kyparissis, A., Levizou, E., Nikolopoulos, D., Petropoulou, Y., Stephanou, M., 1997. The effects of UV-B radiation on European heathland species. Plant Ecol. 128, 252–264.

Bodecker, G.E., McKenzie, R.L., 1996. An algorithm for inferring surface UV irradiance including cloud effects. J. Appl. Meteorol. 35, 1860–1877.

Booth, C.R., 1992–2000. NSF UV Radiation Monitoring Network, Vol. 1–9, Biospherical Instruments Inc., San Diego, CA, USA.

Booth, C.R., Ehramjian, J.C., Mestechkina, T., Cabasug, L.W., Robertson, J.S., Tusson, J.R., 1998. NSF Polar programs UV spectroradiometer network 1995–1997 operations report, Biospherical Instruments Inc., San Diego, CA, 241 pp.

Cabrera, S., Pizarro, G., 1994. Changes in chlorophyll *a* concentration, copepod abundance and UV and PAR penetration in the water column during the ozone depletion in Antarctic Lake Kitiesh, 1992. In: Williamson, C.E., Zagarese, H.E. (Eds.), Archiv. Fur Hydrobiologie. Ergebnisse de Limnologie 43, 71–99.

Caldwell, M.M., 1971. Solar UV irradiation and the growth and development of higher plants. In: Giese, A.C. (Ed.), Photophysiology 6, 131–177.

Caldwell, M.M., Flint, S.D., Searles, P.S., 1994. Spectral balance and UV-B sensitivity of soybean: a field experiment. Plant Cell Environ. 17, 267–276.

Cebula, R.P., Hilsenrath, E., Deland, M.T., 1994. Middle ultraviolet solar spectral irradiance measurements, 1985–1992, from SBUV/2 and SSBUV instruments. In: Pap, J.M., Frölich, C., Hudson, H.S., Folanki, S.K. (Eds.), The Sun as Variable Star: Solar and Stellar Variations. Cambridge University Press, Cambridge, UK, pp. 81–88.

Cebula, R.P., Thuillier, G.O., Van Hoosier, M.E., Hilsenrath, E., Herse, M., Brueckner, G.E., Simon, P.C., 1996. Observation of the solar irradiance in the 200–350 nm interval during the Altas-1 mission: a comparison among three sets of measurements—SSBUV, SOLPEC, and SUSIM. Geophys. Res. Lett. 23, 2289–2292.

Cullen, J.J., Neale, P.J., 1997. Effects of ultraviolet radiation on short-term photosynthesis of natural phytoplankton. Photochem. Photobiol. 65, 264–266.

DeFabo, E.C., Noonan, F.P., 1983. Mechanism of immune suppression by ultraviolet irradiation in vivo. I. Evidence for existence of a unique photoprotector in skin and its role in photoimmunology. J. Exp. Med. 158, 84–89.

Díaz, S., Deferrari, G., Martinioni, D., Oberto, A., 2000. Regression analysis of biologically effective integrated irradiances versus ozone, clouds and geometric factors. J. Atm. Solar-Terrestrial Phys. 62, 629–638.

Díaz, S., Nelson, D., Deferrari, G., Camilión, C., 2003. A model to extend spectral and multi-wavelength UV irradiances time series: model development and validation. J. Geophys. Res. 108 (D4), doi:10.1029/2002JD002134.

Eck, T.F., Bhartia, P.K., Kerr, J.B., 1995. Satellite estimation of spectral UVB irradiance using TOMS derived total ozone and UV reflectivity. Geophys. Res. Lett. 22, 611–614.

Fioletov, V.E., McArthur, L.J.B., Kerr, J.B., Wardle, D.I., 2000. Estimation of long-term changes in ultraviolet radiation over Canada. In: Proceedings of the Quadriennial Ozone Symposium, Sapporo, 2000, pp. 231–232.

Grant, W.B., 2002. An estimate of premature cancer mortality in the United States due to inadequate doses of solar ultraviolet-B radiation, a source of vitamin D. Cancer 94 (6), 1867–1875.

Green, A.E.S., Sawada, T., Shettle, E.P., 1974. The middle ultraviolet reaching the ground. Photochem. Photobiol. 19, 251–259.

Helbling, E.W., Villafane, V., Holm-Hansen, O., 1994. Effects of ultraviolet radiation on Antarctic marine phytoplankton photosynthesis with particular attention to the influence of mixing. In: Weiler, C.S., Penhale, P.A. (Eds.), Ultraviolet Radiation in Antarctica: Measurements and Biological Effects. Antarctic Research Series Vol. 62. American Geophysical Union, Washington, DC, pp. 207–226.

Herman, J., 1998. TOMS ADEOS, National Aeronautic and Spatial Administration/Goddard Space Flight Center (NASA/GSFC).

Hunter, J.H., Taylor, J.H., Moser, H.G., 1979. The effect of ultraviolet irradiation on eggs and larvae of the Northern Anchovy, *Engraulis mordax*, and the Pacific Mackerel, *Scomber japonicus*, during the embryonic stage. Photochem. Photobiol. 29, 325–338.

Ito, T., Sakoda, Y., Uekubo, T., Naganuma, H., Fukuda, M., Hayashi, M., 1994. Scientific application of UV-B observations from JMA network. In: Proceedings of the 13th UOEH International Symposium and the 2nd Pan Pacific Cooperative Symposium on Human Health and Ecosystems. UOEH, Kitakyushu, Japan, pp. 140–142.

Kripke, M.L., Cox, P.A., Alas, L.G., Yarosh, D.B., 1992. Pyrimidine dimmers in DNA initiate systemic suppression in UV-irradiated mice. Proc. Natl. Acad. Sci. U.S.A. 89, 7516–7520.

Li, Z., Wang, P., Cihlar, J., 2000. A simple and efficient method for retrieving surface UV radiation dose rate from satellite. J. Geophys. Res. 105 (4), 5027–5036.

Mc Kinlay, A.F., Diffey, B.L., 1987. A reference action spectrum for ultra-violet induced erythema in human skin, human exposure to ultraviolet radiation: risks and regulations. In: Passchler, W.R., Bosnajanovic, B.M.F. (Eds.). Amsterdam, Elsevier, pp. 83–87.

Mc Peters, R., Beach, E., 1996. TOMS Nimbus-7 and Meteor-3, version 7. National Aeronautic and Spatial Administration/Goddard Space Flight Center (NASA/GSFC).

Mc Peters R., Beach, E., 2001. TOMS Earth Probe. National Aeronautic and Spatial Administration/Goddard Space Flight Center (NASA/GSFC).

Mc Carty, C.A., Taylor, H.R., 1996. Recent developments in vision research. Invest. Ophthalmol. Visual Sci. 37, 1720–1723.

Merriam, J.C., 1996. The concentration of light in the human lens. Trans. Am. Ophthalmol. Soc. 94, 804–918.

Neale, P.J., Davis, R.F., Cullen, J.J., 1998. Interactive effects of ozone depletion and vertical mixing on photosynthesis of Antarctic phytoplankton. Nature 392, 585–589.

Nelson, D.W., 2000. The NOAA Climate Monitoring and Diagnostic Laboratory Solar Radiation Facility, NOAA Technical Memo, OAR CMDL, p. 15.

Rousseaux, M.C., Ballaré, C.L., Giordano, C.V., Scopel, A.L., Zima, A.V., Szwarcberg-Bracchitta, M., Searles, P.S., Caldwell, M.M., Díaz, S.B., 1999. Ozone depletion and UV-B radiation: impact on plant DNA damage in southern South-America. PNAS 96 (26), 15310–15315.

Rozema, J., van de Staaij, J.W.M., Tosserams, M., 1997. Effects of UV-B radiation on plants from agro- and natural ecosystems. In: Lumsden, P.J. (Ed.), Plants and UV-B: Responses to Environmental Change. Cambridge University Press, Cambridge, pp. 213–232.

Searles, P.S., Flint, S.D., Díaz, S.B., Rousseaux, M.C., Ballare, C.L., Caldwell, M.M., 1999. Solar ultraviolet-B radiation influence on sphagnum and carex fen ecosystems: first field season findings in Tierra del Fuego, Argentina. Global Change Biol. 5, 225–234.

Setlow, R.B., 1974. The wavelengths in sunlight effective in producing skin cancer: a theoretical analysis. Proc. Natl. Acad. Sci. U.S.A. 71, 3363–3366.

Sliney, D.H., Wood, R.L., Moscato, P.M., Marshall, W.J., Eriksen, P., 1990. Ultraviolet exposure in the outdoor environment: measurements of ambient ultraviolet exposure levels at large zenith angles. In: Grandolfo, M., et al. (Eds.), Light, Lasers and Synchrotron Radiation. Plenum Press, New York, pp. 169–180.

Smith, R.C., Prezelin, B.B., Baker, K.S., Bidegare, R.R., Boucher, N.P., Colery, T., Karentz, D., MacIntyre, S., Matlick, H.A., Menzies, D., Ondrusek, M., Wan, Z., Waters, K.J., 1992. Ozone depletion: ultraviolet radiation and phytoplankton biology in Antarctic waters. Science 255, 952–959.

Sommaruga, R., Oberleiter, A., Psenner, R., 1996. Effect of UV radiation on the bacterivory of a heterotrophic nanoflagellate. Appl. Environ. Microbiol. 62, 4395–4400.

Teramura, A.H., Sullivan, J.H., 1994. Effects of UV-B radiation on photosynthesis and growth of terrestrial plants. Photosynthesis Res. 39, 463–473.

Tevini, M., 1993. Effects of enhanced UV-B radiation on terrestrial plants. In: Tevini, M. (Ed.), UV-B Radiation and Ozone Depletion: Effects on Humans, Animals, Plants, Microorganisms, and Materials. Lewis Publishers, Boca Raton, Florida, pp. 125–153.

Vernet, M., Smith, R.C., 1997. Effects of ultraviolet radiation on the pelagic Antarctic ecosystem. In: Häder, D.-P. (Ed.), The effects of Ozone Repletion on Aquatic Ecosystems. Environmental Intelligence Unit. Academic Press and R.G. Landes Company, Austin, pp. 247–265.

Vincent, W.F., Roy, S., 1993. Solar ultraviolet radiation and aquatic primary production: damage, protection and recovery. Environ. Rev. 1, 1–12.

Williamson, C., 1995. What role does UV-B radiation play in freshwater ecosystems? Limnol. Oceanogr. 40, 386–392.

WMO, 1999. Chapter 4: Ozone Variability and Trends. WMO/UNEP, Scientific Assessment of Ozone Depletion: 1998. World Meteorological Organization Global Ozone Research and Monitoring Project, Report No. 44, Geneva.